11 INOUE, K.: 'Observation of crosstalk due to four-wave mixing in a laser amplifier for FDM transmission', *Electron. Lett.*, 1987, **23**, pp. 1293–1295
12 JOPSON, R. M., DARCIE, T. E., GAYLIARD, K. T., KU, R. T., TENCH, R. E., RICE, T. C., and OLSSON, N. A.: 'Measurement of carrier-density mediated intermodulation distortion in an optical amplifier', *ibid.*, 1987, **23**, pp. 1394–1395

PULSED LASER EMISSION AT 2·3 μm IN A THULIUM-DOPED FLUOROZIRCONATE FIBRE

Indexing terms: Lasers and laser applications, Optical fibres, Optical properties of substances

We report for the first time laser emission at 2·3 μm from a thulium-doped fluorozirconate fibre pumped by a pulsed alexandrite laser at 0·786 μm. Threshold occurs at 25 μJ incident on the focusing lens. This wavelength is in the 2–3 μm ultra-low loss region of fluorozirconate fibres. Further improvement is expected to result in CW operation using diode laser pumping.

The first observation of laser action from the trivalent thulium $^3H_4 \rightarrow {}^3H_5$ transition at 2·25 μm in a bulk fluorozirconate (ZBLAN) glass[1] was reported recently by our group. We now report the first demonstration of laser action in a ZBLAN fibre at 2·3 μm. The minimum transmission losses for ZBLAN fibres occur over the wavelength region between 2 and 3 micron. This transition at 2·3 μm could therefore be quite useful for developing ultra-low-loss fibre optical communications systems using thulium fibre lasers and amplifiers at this wavelength.

A simplified thulium energy level diagram is shown in Fig. 1. The fluorescent lifetime of the $^3H_4$ upper laser level is

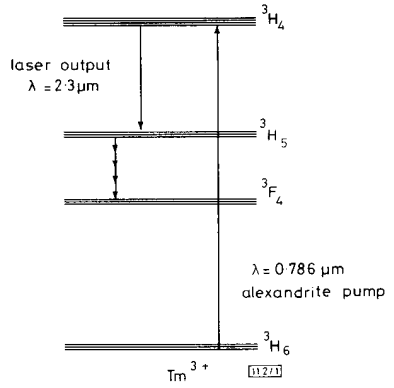

Fig. 1 *Energy level diagram of trivalent thulium, indicating 2·3 μm lasing transition*

For simplicity, only levels relevant to laser transition are shown

1·55 ms as determined by pulsed decay measurements of a bulk glass sample with a thulium concentration of 0·1%. The $^3H_5$ lower laser level lifetime is rapidly quenched via non-radiative multiphonon decay (a few microseconds) to the $^3F_4$ level. As a result, this transition meets the criteria of a classic four-level laser and CW laser emission should therefore be achieved using an appropriate pump source. The onset of pulsed laser emission at 2·3 μm was observed with 25 μJ incident on the microscope objective. CW lasing in this set-up should therefore occur at 16 mW since the threshold pump power for a four-level system is given by the pulsed threshold divided by the fluorescent lifetime.

A block diagram of the experimental set-up is shown in Fig. 2. The ZBLAN fibre was doped with 0·1% trivalent thulium and had a core diameter of 15 μm, a cladding diameter of 150 μm and a numerical aperture of 0·122. A 50 cm length fibre with cleaved ends was inserted between flat

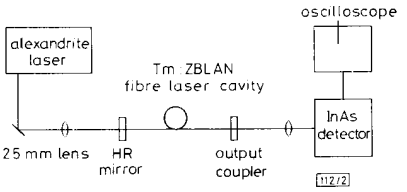

Fig. 2 *Experimental set-up for demonstration of pulsed laser emission from trivalent thulium in fluorozirconate fibre*

mirrors for measuring laser performance. The fibre laser mirror at the input end was butted against the end of the fibre to minimise losses for the fibre resonator. The output mirror was also butted against the other end of the fibre and this arrangement formed the fibre laser resonator. No index matching fluids were used. The input mirror had a high transmissivity (0·85) at the pump wavelength and a high reflectivity (greater than 99%) at the laser wavelength. The output mirror had a transmissivity of 0·5% at the laser wavelength. The pump beam was coupled into the fibre core using a 25 mm microscope objective. The single mode alexandrite laser pump source had a pulsewidth of 200 μs and a repetition rate of 10 Hz. The pump source was tuned to 786 nm to match the absorption peak of the $^3H_6 \rightarrow {}^3H_4$ transition (in our labelling scheme $^3H_4$ is the third excited state in trivalent thulium). A commercial pyroelectric energy detector was used to measure energy of the pump beam and an indium arsenide infra-red detector was used to measure emission from the fibre in the 1–3 micron wavelength region.

In summary we have obtained, for the first time, pulsed room temperature laser operation in a thulium fibre. CW operation using diode laser pumping is anticipated in future work. The authors would like to thank R. J. Ginther for supplying the fluorzirconate material.

L. ESTEROWITZ
R. ALLEN
I. AGGARWAL

Naval Research Laboratory
4555 Overlook Avenue, SW
Washington, DC 20375-5000, USA

21st July 1988

Reference

1 ESTEROWITZ, L., ALLEN, R., KINTZ, G., AGGARWAL, I., and GINTHER, R.: 'Laser emission in Tm^{3+} and Er^{3+}-doped fluorozirconate glass at 2·25, 1·88, and 2·70 μm'. CLEO'88, 28th April 1988, paper ThH1

NEW DETERMINATION OF RESONANT FREQUENCY OF CIRCULAR DISC MICROSTRIP ANTENNA: APPLICATION TO THICK SUBSTRATE

Indexing terms: Antennas, Antenna theory, Microstrip, Resonance

An analytical expression is presented for the resonant frequency of a circular disc microstrip antenna with a thick dielectric substrate. It shows explicitly the dependence of the resonant frequency on the characteristic parameters of a patch antenna. The theoretical results are in good agreement with experimental data.

Introduction: Several methods have been reported in the literature to calculate the resonant frequency of microstrip patch antenna using the cavity model. However, the design formulae

to calculate the circular patch resonant frequency are only accurate for thin substrates of the order of $H/\lambda \leq 0{\cdot}02$ where H is the thickness of the dielectric substrate and λ is the wavelength in the substrate.[1,2]

In previous work,[3] we successfully introduced the dynamic permittivity constant[4] to compute the input impedance of coax-fed rectangular microstrip patch antennas. In this letter, an analytical formula is derived for the resonant frequency of a circular disc microstrip patch antenna with a thick substrate, using this dynamic permittivity constant and a new effective radius.[5]

Model: The circular disc microstrip antenna consists of a planar, resonant radiator of radius a, which is parallel to the ground plane and is separated from the ground plane by a thin layer of dielectric with relative permittivity constant ε_r and thickness H (Fig. 1). The resonant frequencies of the TM modes in the circular disc microstrip antenna are given as:

$$r_{nm} = \frac{\alpha_{nm} \cdot C_0}{2 \cdot \pi \cdot a_{eff} \cdot \sqrt{(\varepsilon_{dyn})}} \tag{1}$$

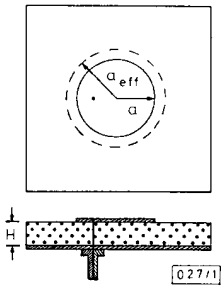

Fig. 1 *Geometry of circular microstrip antenna*

where c_0 is the velocity of light in vacuum, α_{nm} is the mth zero of the derivative of the Bessel function of order n. The dominant mode is the TM_{11} mode which has the lowest resonant frequency where $\alpha_{11} = 1{\cdot}84118$. ε_{dyn} is the dynamic permittivity constant given by the formula of Wolff and Knoppik,[4] in which we replace the static fringing capacitance by the one given by Chew and Kong:[5]

$$C = \frac{a^2 \pi \varepsilon_r \varepsilon_0}{H}\left\{1 + \frac{2H}{\pi \varepsilon_r a}\left[L_n\left(\frac{a}{2H}\right) + (1{\cdot}41\varepsilon_r + 1{\cdot}77) + \frac{H}{a}(0{\cdot}68\varepsilon_r + 1{\cdot}65)\right]\right\} \tag{2}$$

a_{eff} is an effective radius slightly larger than the physical one taking into account the influence of the fringing field at the edges, and the dielectric inhomogeneity of the circular disc microstrip patch antenna.[4] Chew and Kong[5] have studied this influence of the fringing field by a seminumerical approach, and from expr. 2 we can define an effective radius a_{eff} which is valid for $H/a \leq 0{\cdot}5$ and $\varepsilon_r < 10$. It is given by:

$$a_{eff} = a\left\{1 + \frac{2H}{\pi \varepsilon_r a}\left[L_n\left(\frac{a}{2H}\right) + (1{\cdot}41\varepsilon_r + 1{\cdot}77) + \frac{H}{a}(0{\cdot}68\varepsilon_r + 1{\cdot}65)\right]\right\}^{1/2}$$

Results: The lowest resonant frequency f_{11} calculated using the design formula presented here is compared with that of Howell,[2] Wolff *et al.*,[4] and Derneryd[6] in Table 1. We observe that our results fall among those calculated by the other three methods, and are closer to measured values in most cases. Fig. 2 presents the normalised resonant frequencies plotted as a function of electrical thickness. A normalised resonant frequency is defined as $f_n = f_{11}/f_H$ where f_H is the zeroth-order prediction of the resonant frequency $f_H = (1{\cdot}84118 \cdot C_0)/(2 \cdot \pi \cdot a \cdot \sqrt{(\varepsilon_r)})$.

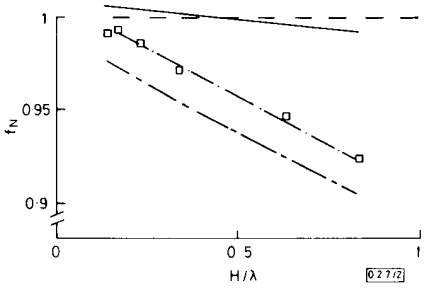

Fig. 2 *Calculated and measured normalised resonant frequencies*
$\varepsilon_r = 4{\cdot}55$, $H = 2{\cdot}35$ mm
---- Howell
——— Wolff
□□□ experimental
–·–·– best fit to experimental data
—·— Derneryd

The agreement between our theoretical and experimental values of the resonant frequency is typically within 0·5% for values of electrical thickness $H/\lambda \sim 0{\cdot}1$.

Acknowledgment: The authors wish to thank CNET (La Turbie, France) for experimental support during this study.

F. ABBOUD
J. P. DAMIANO
A. PAPIERNIK
Laboratoire d'Electronique—GRECO Microantennes du CNRS
Université de Nice
Parc Valrose, 06034 Nice Cédex, France

12th July 1988

Table 1 COMPUTED AND MEASURED RESONANT FREQUENCIES

a	H	ε_r	H/λ	Measured	Howell[2]	Wolff[4]	Derneryd[6]	Our model
cm	mm			GHz	GHz	GHz	GHz	GHz
3·493	1·588	2·50	0·013	1·570*	1·580	1·569	1·537	1·556
1·270	0·794	2·59	0·018	4·070*	4·290	4·267	4·159	4·175
3·493	3·175	2·50	0·025	1·510*	1·580	1·526	1·478	1·522
13·894	12·700	2·70	0·026	0·378*	0·387	0·362	0·350	0·370
4·950	2·350	4·55	0·014	0·825	0·833	0·836	0·814	0·827
3·975	2·350	4·55	0·017	1·030	1·037	1·042	1·009	1·027
2·990	2·350	4·55	0·023	1·360	1·379	1·384	1·332	1·358
2·000	2·350	4·55	0·034	2·003	2·061	2·067	1·965	2·009
1·040	2·350	4·55	0·063	3·750	3·963	3·950	3·661	3·744
0·770	2·350	4·55	0·083	4·945	5·353	5·308	4·848	4·938

* These first four frequencies have been measured by Howell[2] and we have measured the others

References

1 WATKINS, J.: 'Circular resonant structures in microstrip', *Electron. Lett.*, 1969, **5**, pp. 524–525
2 HOWELL, J. Q.: 'Microstrip antenna', *IEEE Trans.*, 1975, **23**, pp. 90–93
3 ABBOUD, F., DAMIANO, J. P., and PAPIERNIK, A.: 'A simple model for the input impedance of coax-fed rectangular microstrip patch antenna for C.A.D.', to be published in *IEE Proc. H*, Oct. 1988, **135**, no. 5
4 WOLFF, I., and KNOPPIK, N.: 'Rectangular and circular microstrip disk capacitors and resonators', *IEEE Trans.*, 1974, **MTT-22**, pp. 857–864
5 CHEW, W. C., and KONG, J. A.: 'Effects of fringing field on the capacitance of circular microstrip disk', *IEEE Trans.*, 1980, **MTT-28**, pp. 98–104
6 DERNERYD, A. G.: 'Microstrip disc antenna covers multiple frequencies', *Microwave J.*, May 1978, pp. 77–79

140 Mbit/s DPSK TRANSMISSION USING AN ALL-OPTICAL FREQUENCY CONVERTOR WITH A 4000 GHz CONVERSION RANGE

Indexing terms: Optical communications, Frequency convertors, Mixers, Optical frequency conversion, Four-wave-mixing, Optical amplifiers

A new method of optical frequency conversion is described and demonstrated by a 140 Mbit/s DPSK optical transmission experiment. A modulated optical input signal is converted by 1500 GHz in a modulated optical output signal with a fibre-to-fibre efficiency of −10 dB.

Introduction: Optical frequency conversion is important for future coherent optical multichannel switching networks.[1] However, to our knowledge, no optical transmission experiment using frequency conversion has been reported. A possible means for frequency conversion is nearly degenerate four-wave-mixing (NDFWM) in semiconductor laser optical amplifiers.[2–5] In a conventional NDFWM experiment a signal wave S_{in} and a pump wave P_1 both travelling with the same polarisation in the same direction through a semiconductor optical amplifier (OA) generate two new light waves FW1 and FW2 as indicated in Fig. 1. If S_{in} is modulated and P_1 unmodulated, we obtain from calculations and experiment that FW2

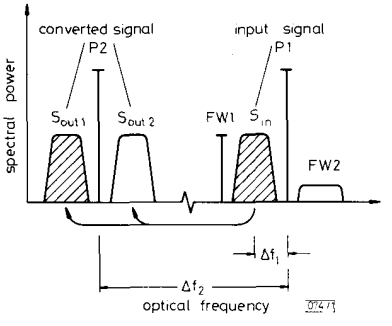

Fig. 1 *Schematic diagram of light spectrum at output of semiconductor optical amplifier*

In experiment we used $\Delta f_1 = 1$ GHz and $\Delta f_2 = 1500$ GHz

is a frequency-converted replica of S_{in}, whereas FW2 degenerates to a δ-function (for PSK modulation). This scheme of frequency conversion has the disadvantage that the frequency spacing $2\Delta f_1$ between the input signal S_{in} and the frequency-converted signal FW2 is limited to less than 5 GHz by the efficiency of NDFWM in an OA.[3–5] Here Δf_1 is the frequency spacing between P_1 and S_{in}. To enlarge this frequency spacing we used a second pump wave P_2 (see Fig. 1). The resulting spectrum of the input and generated waves, which is shown schematically in Fig. 1, is only valid if the frequency spacing Δf_2 between P_1 and P_2 is larger than 20 GHz. The power of the generated light waves S_{out1} and S_{out2} is proportional to the product of the powers of P_2, P_1 and S_{in}, and are located with a frequency spacing Δf_1 at each side of P_2, S_{out1} and S_{out2} are each a frequency-converted replica of the input signal S_{in}. In contrast to the strong dependence of the NDFWM efficiency on Δf_1, S_{out1} and S_{out2} are only weakly dependent on Δf_2. Therefore the frequency conversion range Δf_2 can be as large as 4000 GHz (the 3 dB bandwidth of our OA). In this letter we demonstrate the successful all-optical frequency conversion with the use of 140 Mbit/s DPSK signal transmission.

Experiment: The experimental set-up is schematically depicted in Fig. 2. Three tunable external-cavity semiconductor lasers

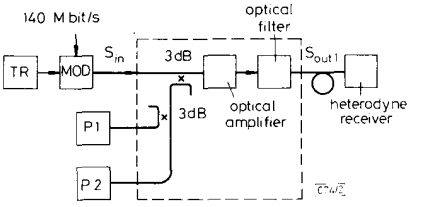

Fig. 2 *Schematic diagram of experimental set-up*

(1·3 μm, spectral width less than 100 kHz, equipped with isolators) provide the light waves P_1, P_2 and S_{in}. The frequency spacings are $\Delta f_1 = 1$ GHz between S_{in} and P_1 and $\Delta f_2 = 1500$ GHz between P_1 and P_2. The light wave S_{in} is modulated by a $LiNbO_3$ phase modulator with a 140 Mbit/s DPSK signal. The three light waves are fed via fibre couplers into an OA with input light powers 14·5 μW, 28 μW and 1·2 μW for P_1, P_2 and S_{in} respectively. The OA (an AR-coated Hitachi HLP 5400 laser) exhibits an internal TE single-pass gain of 21 dB with a gain ripple of less than 2 dB. The OA output waves are indicated schematically in Fig. 1. With the data given above the converted signal power S_{out1} at the output of the OA is 3 μW. An optical filter (grating) following the OA transmits the light components S_{out1}, S_{out2} and P_2 with a loss of 2 dB and suppresses the light components P_1, S_{in}, FW1 and FW2 by at least 50 dB. The local laser of the heterodyne receiver is tuned to select the converted signal S_{out1} (intermediate frequency 1·5 GHz, seven-stage Chebyshev filter). Transmission experiments with a BER of 10^{-9} were performed. Fig. 3 shows an eye diagram of the received DPSK signal. If we consider the frequency convertor as defined by all components inside the broken line in Fig. 2, the fibre-to-fibre conversion efficiency of S_{in} to S_{out1} is better than −10 dB.

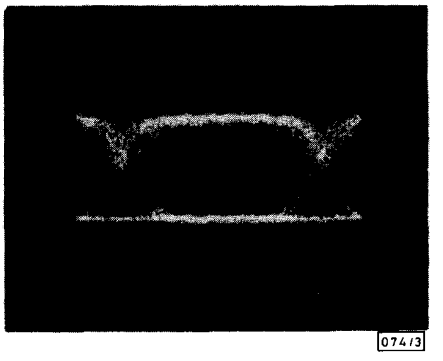

Fig. 3 *Eye diagram of received DPSK signal*

Conclusion: All-optical frequency conversion of 1500 GHz was realised with a fibre-to-fibre efficiency of −10 dB. The converted signal was received by a heterodyne receiver with a BER of 10^{-9}. The efficiency of NDFWM requires that the frequency separation Δf_1 between S_{in} and P_1 and consequently also between S_{out1} and P_2 is less than 2·5 GHz. This restricts the data rate in our system. On the other hand P_1 and P_2 can be set arbitrarily with respect to the 4000 GHz bandwidth of